

Response surface methodology-based optimization of cellulase production by *Trichoderma asperelloides* RS1 through solid-state fermentation using coconut coir

Jhoanna Mae A. Minion¹, Leo Joseph F. Labitag², Annie Cita T. Kagaoan², Adonis A. Yanos¹, Sheryl Lozel B. Arreola¹, and Nico G. Dumandan*²

¹Institute of Chemistry, College of Arts and Sciences, University of the Philippines Los Baños, College 4031, Laguna

²National Institute of Molecular Biology and Biotechnology, University of the Philippines Los Baños, College 4031, Laguna

ABSTRACT

This study optimized cellulase production from *Trichoderma asperelloides* RS1 using coconut coir as a substrate through solid-state fermentation. A Box-Behnken response surface methodology was employed to optimize three independent factors: fermentation time (3, 6.5, and 10 days), initial media pH (4, 6, and 8), and initial moisture content (80%, 140%, and 200%). Response surface methodology showed significant models for FPase and CMCase activities with p-values <0.0001. Optimal

FPase activity (0.762 U_{glc/gds}) was achieved at pH 6.0, 140% moisture, and 6.5 days. The highest CMCase activity (0.295 U_{glc/gds}) occurred after 3 days at pH 8.0 and 140% moisture. The regression model showed strong agreement between predicted and actual cellulase activities, with percent errors of 0.74% and 1.83% for FPase and CMCase, respectively.

INTRODUCTION

The Philippines is considered one of the leading producers of coconut globally, contributing significantly to the world's coconut industry (Rodriguez et al. 2017). Often referred to as the "Tree of Life", coconut offers a variety of products derived from

*Corresponding author

Email Address: ngdumandan@up.edu.ph

Date received: October 22, 2024

Date revised: November 28, 2024

Date accepted: January 3, 2025

DOI: <https://doi.org/10.54645/2025181GGL-47>

KEYWORDS

Trichoderma asperelloides, cellulase, coconut coir, response surface methodology, solid state fermentation

its various parts, including coconut fruit, water, oil, and milk. Coconut husk constitutes forty percent (40%) of the fruit, where the fibrous outer layer called coconut coir represents a substantial by-product of the coconut industry. According to Khalil et al. (2006), the coir's composition is approximately 44% cellulose, 33% lignin, 12% hemicellulose, 6% extractives, and 2% ash. Traditionally utilized for crafting ropes, brushes, padding, and floor mats (Ali et al. 2022), coconut coir has garnered attention for its potential in modern industrial applications, yet comprehensive studies exploring its utilization for enzyme production remain scarce.

Cellulase enzymes are essential for facilitating the breakdown of cellulose into simpler sugars, making them vital for applications in biofuel production, textile processing, and the food and beverage industry (Campos et al. 2024). Their versatility and importance are underscored by their substantial contribution to the global enzyme market, which accounts for 8% of industrial demand (Poddar et al. 2017). These enzymes are primarily derived from filamentous fungi, such as *Aspergillus* spp. and *Trichoderma* spp., which are adept at producing complex enzymes like cellulases (Keshavarz and Khalesi 2016; Peij et al. 1998; Phitsuwan et al. 2013). *Trichoderma* species are often used in biofuel industries due to their ability to produce highly active cellulase systems that hydrolyze polymers present in lignocellulosic agricultural wastes like cellulose, hemicellulose, lignin, and chitin (Druzhinina et al. 2018).

Enzymes are industrially produced through submerged fermentation (SmF), which utilizes liquid substrates for the fermentation of specific microorganisms (Ouedraogo and Tsang 2021). Typical enzyme production methods often face challenges related to cost, sustainability, and efficiency. This underscores the need for exploring alternative substrates and fermentation techniques to enhance enzyme production economically and sustainably.

Solid-state fermentation (SSF) is increasingly recognized as a viable approach in this context. Unlike submerged fermentation, SSF facilitates microbial growth on solid substrates under conditions with limited or no free water, offering distinct advantages for various bioprocesses. This method offers several advantages for enzyme production, including higher product concentrations, reduced water usage, and the ability to utilize agricultural and industrial residues effectively (Abu Yazid et al. 2017). Harnessing SSF could potentially overcome limitations associated with traditional fermentation methods, thereby enhancing the efficiency and sustainability of cellulase production. In addition, filamentous fungi have advantages on SSF as they can thrive in various solid substrates with diverse conditions, such as low water content (Hewedy et al. 2020).

Transitioning to SSF through filamentous fungi for cellulase production using coconut coir presents substantial potential. The fibrous nature of coconut coir creates an optimal environment for fungal growth and enzymatic activity under solid-state conditions. This aligns closely with ongoing efforts to leverage lignocellulosic biomass in advancing industrial biotechnology applications. Thus, this study aims to investigate the viability of utilizing coconut coir in SSF for cellulase production by *Trichoderma asperelloides* RS1. Through the optimization of fermentation parameters using Response Surface Methodology (RSM), the study endeavors to improve cellulase production efficiency from coconut coir. This study contributes to advancing sustainable practices in enzyme biotechnology by exploring the potential of cellulase-producing *Trichoderma asperelloides* using coconut coir as a substrate via SSF.

MATERIALS AND METHODS

Materials and microorganism

Coconut coir fibers were sourced from fresh coconut husks collected in San Andres, Catanduanes, Philippines. All chemicals and reagents utilized in this study were of analytical grade and procured from commercial suppliers.

Trichoderma sp. RS1 was the microorganism used in this study. It was isolated from rice straw and maintained at the Feeds and Specialty Products Laboratory, BIOTECH, UPLB, Laguna, Philippines. The pure cultures were preserved on potato dextrose agar (PDA) slants at 4°C for short-term storage. For long-term storage, spore suspensions were prepared in a 1:1 (v/v) glycerol solution and kept at -20°C.

Molecular identity confirmation of fungi

The genomic DNA of *Trichoderma* sp. RS1 was extracted using the InstaGene™ Matrix (Bio-Rad, California, USA) via the boiling method. Isolated fungal tissues were transferred into duplicate microcentrifuge tubes and resuspended in 1 mL of sterile water. The suspension was centrifuged at room temperature for 2 min at 10,000 rpm to collect the pellet. The supernatant was discarded, and 200 µL of InstaGene™ Matrix was added to each pellet. The samples were incubated at 56°C for 30 min with shaking using a thermal mixer. Following incubation, the tubes were vigorously shaken for 10 s using a vortex mixer and then placed in a heat block at 100°C for 8 min. After boiling, the samples were centrifuged again at 10,000 rpm for 5 min at room temperature. The supernatant containing the isolated genomic DNA was carefully collected and transferred to sterile cryovials for storage at -20°C. The quality and integrity of the extracted DNA were assessed by measuring the absorbance ratio at 260 nm and 280 nm using a NanoDrop (Thermo Fisher Scientific, Massachusetts, USA) spectrophotometer.

The internal transcribed spacer (ITS) region was amplified using standard ITS5 (5'-GGAAGTAAAAGTCGTAACAAGG-3') and ITS4 (5'-TCCTCCGCTTATTGATATGC-3') primers (Macrogen, Inc., South Korea). The PCR parameters used were: (1) initial denaturation at 95°C for 5 min; (2) 31 cycles of denaturation at 95°C for 0.5 min, annealing at 57°C for 0.5 min, and extension at 72°C for 1.4 min; and (3) final extension at 72°C for 10 min. The amplified ITS regions were submitted to Macrogen, Inc. for purification and sequencing. The obtained ITS region sequences were compared with reference sequences using the Basic Local Alignment Search Tool (BLAST) to confirm fungal identification.

Trichoderma sp. inoculum preparation

The inoculum used in SSF was prepared by adding 10 mL of 0.9% (w/v) sterile NaCl solution to the fungal strain grown in PDA slant to harvest the spores. The spore suspension was then collected and standardized using a hemocytometer to obtain a final spore count of 10^7 per mL.

SSF optimization of cellulase production by response surface methodology

The Box-Behnken design (BBD), generated using Design-Expert® DX13 software (Stat-Ease, Inc., Minnesota, USA), was employed to optimize the fermentation time (days), initial media pH, and initial moisture content (%) of the substrate (Table 1). This optimization aimed to enhance cellulase production by *Trichoderma* sp. during SSF, utilizing coconut coir as the substrate.

Table 1: Independent variables and their factorial levels used in the optimization of cellulase production.

Factor	Factorial Levels		
	-1	0	+1
Fermentation time, days	3	6.5	10
Initial pH of fermentation medium	4	6	8
Initial moisture content of substrate, %	80	140	200

(-1) - low level factorial; (0) - mid level factorial; (+1) - high level factorial

These independent variables were studied at three levels with five replicates at the center point with a total of seventeen experimental runs. A second-order polynomial equation was applied for the analysis of cellulase activity, and the data were fitted into the second-order polynomial equation according to Equation 1.

$$Y = \beta_0 + \beta_1\chi_1 + \beta_2\chi_2 + \beta_3\chi_3 + \beta_{12}\chi_1\chi_2 + \beta_{13}\chi_1\chi_3 + \beta_{23}\chi_2\chi_3 + \beta_1^2\chi_1^2 + \beta_2^2\chi_2^2 + \beta_3^2\chi_3^2$$

Equation 1

where Y is the predicted response (cellulase activity); χ_1 , χ_2 , and χ_3 are the fermentation time, initial media pH, and initial moisture content, respectively; β_0 is an intercept; β_1 , β_2 , and β_3 are the linear coefficients; β_{12} , β_{13} , and β_{23} are the interaction coefficients; β_1^2 , β_2^2 , and β_3^2 are the quadratic coefficients.

Cellulase production via SSF was carried out in 500-mL Erlenmeyer flasks containing 5.0 g of the prepared coconut coir substrate. The fermentation medium (300 g/L glucose, 150 g/L KH_2PO_4 , 5.0 g/L $(\text{NH}_4)_2\text{SO}_4$, 1.0 g/L $\text{MgSO}_4 \cdot 7\text{H}_2\text{O}$, 1.0 g/L NaCl, 5.0 mg/L $\text{FeSO}_4 \cdot 7\text{H}_2\text{O}$, 1.6 mg/L MnSO_4 , 3.45 mg/L $\text{ZnSO}_4 \cdot 7\text{H}_2\text{O}$, and 2.0 mg/L $\text{CoCl}_2 \cdot 6\text{H}_2\text{O}$ adjusted to the desired pH using either 1.0 N HCl or 1.0 N NaOH) was added to the substrate to achieve the target moisture content based on experimental parameters. The moistened substrate was then sterilized at 121°C for 15 min, and subsequently inoculated with 1.0 mL of the prepared inoculum. Fermentation proceeded at room temperature for varying durations according to the experimental setup.

Enzyme extraction and activity assay

After fermentation, the contents of each flask were mixed with 45 mL of 0.2 M sodium acetate buffer at pH 4.8 to extract the crude cellulase (Pirota et al. 2013). The flasks were gently shaken at room temperature for 10 min, and the solid residue was separated from the extract by filtering through gauze, followed by centrifugation at 10,000 rpm at 4°C for 20 min. The supernatant was taken as a crude enzyme extract and stored at 2°C until further analysis.

Cellulase activity was evaluated using two assays: the filter paper (FPase) assay for total cellulolytic activity and the carboxymethyl cellulose (CMCase) assay for endoglucanase activity, following the method described by Ryu and Mandels (1980).

For the FPase assay, a strip of filter paper (1 cm x 6 cm, 50.0 mg) was placed in a tube and saturated with 1.0 mL of 0.05 M sodium citrate buffer (pH 4.8). Subsequently, 0.5 mL of crude enzyme extract was added to the tube and incubated exactly for 1 h at 50°C. For the CMCase assay, a 0.5 mL aliquot of enzyme was added to 0.5 mL of 2% w/v CMC in 0.05 M sodium acetate buffer (pH 5.0). The reaction was allowed to proceed by incubating at 50°C for exactly 30 min.

The reactions for all assays were stopped by heating at 100°C for 5 min, followed by the addition of 100 μL of 1% w/v 3,5-dinitrosalicylic acid reagent (in 0.5 N NaOH) to a 100 μL aliquot of the reaction mixture. The final mixture was then heated at

100°C for 10 min to allow color development, which was read using a spectrophotometer at 540 nm absorbance. The amount of reducing sugar was interpolated from a standard glucose calibration curve, and the activity was calculated using the equation:

$$\text{Enzyme activity} \left(\frac{U_{\text{FPase/CMCase}}}{\text{gds}} \right) = \frac{\left(\frac{A}{V_s} \right) \times \text{DF}}{t}$$

Equation 2

where A is the interpolated reducing sugar (as glucose equivalent in $\mu\text{mol/L}$); m_s is the mass of dried substrate (in g); V_s is the volume of buffer used to extract the enzyme (in L); t is the incubation time (in min); and DF is the dilution factor.

The total cellulolytic activity (U_{FPase}) and endoglucanase activity (U_{CMCase}) units were defined as the amount of enzyme per gram dry substrate (gds) that liberates reducing sugar at a rate of 1.0 $\mu\text{mol/min}$ under the assayed conditions.

Effect of pH and temperature on cellulase activity

The impact of pH and temperature on crude cellulase activity was evaluated by measuring CMCase activity under varying pH and temperature conditions. For the pH assessment, 2% w/v CMC was dissolved in different buffers: 0.050 N sodium acetate buffer adjusted to pH 3.0, 4.0, and 5.0 using either 1.0 N NaOH or 1.0 N HCl, and 0.050 N phosphate buffer adjusted to pH 6.0, 7.0, and 8.0 using 1.0 N NaOH or 1.0 N phosphoric acid. For temperature sensitivity, the reaction mixture containing 2% w/v CMC in the 0.050 N buffer at the determined optimal pH was incubated for 30 min at temperatures ranging from 30°C to 80°C at 10°C increments.

RESULT AND DISCUSSION

Identity and phylogeny of *Trichoderma* sp. RS1

Genomic DNA isolation, ITS region amplification via PCR, and DNA sequencing were conducted to obtain the ITS region sequence of *Trichoderma* sp. RS1. Sequence alignment and phylogenetic analysis identified isolate RS1 as *Trichoderma asperelloides*. Nucleotide BLAST analysis of the ITS region sequence showed that isolate RS1 has a very high similarity of 100% identity to *Trichoderma asperelloides* isolate STAL. The ITS region sequence of isolate RS1 was submitted to the National Center for Biotechnology Information (NCBI) and assigned the accession number PP989906.1.

The phylogenetic tree was generated using sequences retrieved from GenBank, including the following accession numbers: OP821901.1 (Chen 2022), MH371292.1 (Rajyalakshmi et al. 2018), NR_120297.1 (Robbertse et al. 2018a), NR_138435.1 (Robbertse et al. 2018b), NR_134436.1 (Robbertse et al. 2018c), NR_111348.1 (Schoch 2018), and OM280457.1 (Shelke et al. 2022). Phylogenetic analysis of closely related species further confirmed the identification of isolate RS1 as *T. asperelloides*. Figure 1 shows the phylogenetic relationships between *T. asperelloides* RS1 and related species generated using the ClustalW algorithm for multiple sequence alignment and the

Neighbor-Joining method (Maximum Composite Likelihood model) in MEGA 11, with 1000 bootstrap replicates. Analysis of the neighbor-joining tree confirmed the correct classification of isolate RS1 within the *Trichoderma* genus. The high bootstrap value supports the robustness of the branch where *Trichoderma* sp. RS1 clusters with *Trichoderma asperelloides* isolate STAL

and *Trichoderma asperellum* isolate Manik Chaman. This indicates that these three species share a more recent common ancestor compared to the other fungi included in the phylogenetic tree.

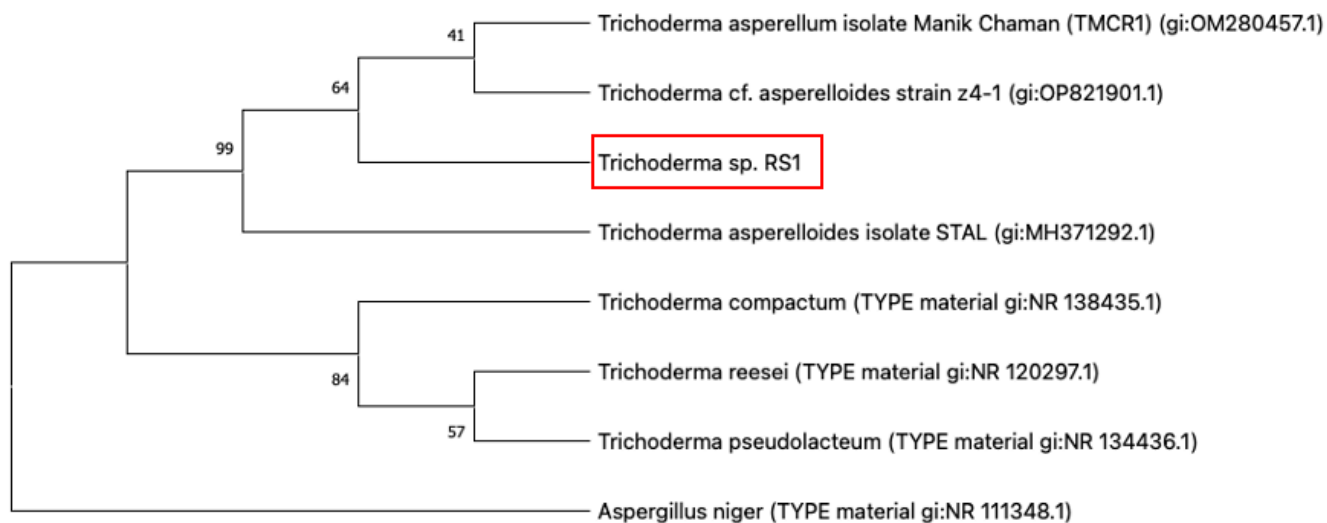


Figure 1: Neighbor-joining tree showing the phylogenetic relationships of ITS region sequences of *Trichoderma asperelloides* RS1 and related species, with *Aspergillus niger* as the outgroup.

SSF optimization of cellulase production by response surface methodology

BBD was utilized in this study to systematically evaluate the effects of the three independent variables (initial pH of fermentation medium, initial moisture content, and fermentation time) on the cellulase production by *T. asperelloides* RS1 via SSF. Using the Design-Expert[®] DX13 software, an experimental

design matrix was generated to explore the interactions between these variables and to identify the conditions that yield the highest cellulase activity (measured as FPase and CMCase). The actual levels of the variables and responses for each experimental run are summarized in Table 2.

Table 2: Box-Behnken design matrix for the optimization of cellulase (FPase and CMCase) production by *T. asperelloides* RS1 via solid-state fermentation using coconut coir.

Run	A	B	C	FPase activity*	CMCase activity*
1	3	6	200	0.665	2.397
2	6.5	6	140	0.735	2.562
3	10	6	200	0.562	1.893
4	6.5	8	200	0.725	2.582
5	6.5	6	140	0.72	2.527
6	6.5	6	140	0.762	2.525
7	6.5	4	200	0.533	1.772
8	3	8	140	0.74	2.951
9	6.5	6	140	0.733	2.515
10	6.5	4	80	0.441	1.12
11	10	4	140	0.507	1.526
12	10	8	140	0.68	2.073
13	6.5	8	80	0.665	1.985
14	3	6	80	0.505	1.707
15	6.5	6	140	0.733	2.349
16	3	4	140	0.507	1.474
17	10	6	80	0.488	1.333

A – fermentation time (days), B – initial media pH, C – initial moisture content (%)
*Expressed as U/g coconut coir (gds)

Based on Table 2, it can be observed that lower FPase activity than the corresponding CMCase activity is obtained given the same fermentation conditions. This observation can be attributed to several factors related to the nature of the enzymes and the substrate used in the assay. β -1,4-endoglucanase, or simply endoglucanase, represented by CMCase activity, primarily cleaves internal β -1,4-glycosidic bonds in cellulose, creating new chain ends and reducing the degree of polymerization of cellulose, making the cellulose more accessible for further enzymatic action (Srivastava et al. 2018, Tomás-Pejó et al.

2009). In contrast, FPase represents the total cellulolytic activity on a more crystalline and complex substrate, like filter paper (Sahin and Arslan 2008). Filter paper is a crystalline form of cellulose, making it harder for cellulases to act upon compared to the more accessible and amorphous CMC used in CMCcase assays. Also, CMC is soluble in water, which allows easier access for endoglucanases, resulting in higher measurable activity. On the other hand, filter paper is insoluble, requiring more synergistic action of different cellulase components, which can reduce the overall observed activity.

To identify the most suitable model for cellulase production, several statistical criteria were assessed, including the Predicted Residual Sum of Squares (PRESS), adjusted R², and predicted R² (Tables 3 and 4). Four models were examined in this study: linear, two-factor interaction (2FI), quadratic, and cubic. The PRESS values for the model optimizing cellulase production measured as FPase activity were 0.1374, 0.2260, and 0.0223, respectively, while the cubic model has a leverage of 1.0000,

wherein PRESS statistics cannot be defined. On the other hand, for the model optimizing cellulase production measured as CMCase activity, the same trend follows where linear, 2FI, and quadratic have 2.43, 3.34, and 0.29 values of PRESS, respectively. Among these, the quadratic model has the lowest PRESS value, suggesting a better model's predictive ability compared to other models.

Table 3: Model summary for the selection of the best-fitting model to optimize cellulase production measured as FPase activity.

Source	Std. Dev.	R ²	Adjusted R ²	Predicted R ²	PRESS	
Linear	0.0844	0.5366	0.4297	0.3119	0.1374	
2FI	0.0946	0.5517	0.2827	-0.1319	0.2260	
Quadratic	0.0179	0.9887	0.9742	0.8881	0.0223	Suggested
Cubic	0.0154	0.9952	0.9810			Aliased

Table 4: Model summary for the selection of the best-fitting model to optimize cellulase production measured as CMCase activity.

Source	Std. Dev.	R ²	Adjusted R ²	Predicted R ²	PRESS	
Linear	0.3487	0.6436	0.5613	0.4515	2.43	
2FI	0.3687	0.6935	0.5095	0.2466	3.34	
Quadratic	0.0790	0.9901	0.9775	0.9339	0.29	Suggested
Cubic	0.0839	0.9937	0.9746			Aliased

The PRESS value serves as a key indicator of a model's ability to predict responses for new data, with lower values reflecting higher predictive accuracy. Along with PRESS, adjusted R² and predicted R² were also used to guide model selection. In both experimental matrices, the quadratic models exhibited high adjusted R² and predicted R² values, suggesting not only a good fit to the data but also strong predictive accuracy (Manikandan et al. 2013). Consequently, the quadratic model was chosen as the best fit for deriving the predictive equation for cellulase production.

Supplementary analysis using ANOVA and sequential model sum of squares determined that the chosen quadratic model was the most fitting. In Tables 5 and 6, the data were used to compare different statistical models to find the best fitting model for the generation of the regression equation for FPase and CMCase activity. Both models showed a high F-value and a *p*-value <0.0001, indicating model terms are significant. These results indicate that the quadratic model significantly explains the variability in cellulase production data with minimal error.

Table 5: Comparison of different statistical models to find the best fitting model for the generation of the regression equation for FPase activity.

Source	Sum of Squares	df	Mean Square	F-value	<i>p</i> -value	
Mean vs Total	6.74	1	6.74			
Linear vs Mean	0.1071	3	0.0357	5.02	0.0158	
2FI vs Linear	0.0030	3	0.0010	0.1119	0.9511	
Quadratic vs 2FI	0.0872	3	0.0291	90.39	< 0.0001	Suggested
Cubic vs Quadratic	0.0013	3	0.0004	1.83	0.2818	Aliased
Residual	0.0009	4	0.0002			
Total	6.94	17	0.4080			

Table 6: Comparison of different statistical models to find the best fitting model for the generation of the regression equation for CMCase activity.

Source	Sum of Squares	df	Mean Square	F-value	<i>p</i> -value	
Mean vs Total	73.26	1	73.26			
Linear vs Mean	2.85	3	0.9513	7.82	0.0031	
2FI vs Linear	0.2212	3	0.0737	0.5425	0.6641	
Quadratic vs 2FI	1.32	3	0.4385	70.26	< 0.0001	Suggested
Cubic vs Quadratic	0.0156	3	0.0052	0.7378	0.5821	Aliased
Residual	0.0281	4	0.0070			
Total	77.70	17	4.57			

ANOVA was also performed to test the statistical significance of the model. It was used to determine whether to include or exclude the coefficients for linear, interaction, and quadratic terms in the model based on their *p*-values. Conversely, if the *p*-value is greater than 0.05, it indicates no significant effect of the varying input levels on the response (Awotwe-Otoo, 2012).

time (AC), and the quadratic terms of moisture content (A²), fermentation time (B²), and initial moisture content (C²) were identified to be significant. In contrast, all model terms in the quadratic model for optimized cellulase production measured as CMCase activity were significant, except for the interaction between fermentation time and initial moisture content (AC) and between initial media pH and moisture content (BC).

Shown in Tables 7 and 8 are the significant terms for the optimization of cellulase production measured as FPase activity and CMCase activity, respectively. For FPase activity, initial moisture content (A), initial media pH (B), fermentation time (C), the interaction between moisture content and fermentation

Table 7: ANOVA and Lack of Fit analysis of the quadratic model for optimized cellulase production measured as FPase activity.

Source	Sum of Squares	df	Mean Square	F-value	p-value
Model	0.1974	9	0.0219	68.17	< 0.0001*
A	0.0040	1	0.0040	12.59	0.0094*
B	0.0845	1	0.0845	262.51	< 0.0001*
C	0.0186	1	0.0186	57.89	0.0001*
AB	0.0009	1	0.0009	2.80	0.1383 ^{ns}
AC	0.0018	1	0.0018	5.75	0.0477 ^{ns}
BC	0.0003	1	0.0003	0.7957	0.4020 ^{ns}
A ²	0.0283	1	0.0283	88.10	< 0.0001*
B ²	0.0089	1	0.0089	27.75	0.0012*
C ²	0.0417	1	0.0417	129.69	< 0.0001*
Residual	0.0023	7	0.0003		
Lack of Fit	0.0013	3	0.0004	1.83	0.2818 ^{ns}
Pure Error	0.0009	4	0.0002		
Cor Total	0.1996	16			

A – fermentation time (days); B – initial media pH; C – initial moisture content (%)

*Significant (p-value <0.05); nsNot significant (p-value >0.05)

Table 8: ANOVA and Lack of Fit analysis of the quadratic model for optimized cellulase production measured as CMCase activity.

Source	Sum of Squares	df	Mean Square	F-value	p-value
Model	4.39	9	0.4879	78.16	< 0.0001*
A	0.3630	1	0.3630	58.15	0.0001*
B	1.71	1	1.71	274.03	< 0.0001*
C	0.7806	1	0.7806	125.07	< 0.0001*
AB	0.2162	1	0.2162	34.64	0.0006*
AC	0.0042	1	0.0042	0.6769	0.4378 ^{ns}
BC	0.0008	1	0.0008	0.1212	0.7380 ^{ns}
A ²	0.2867	1	0.2867	45.93	0.0003*
B ²	0.2202	1	0.2202	35.28	0.0006*
C ²	0.6810	1	0.6810	109.11	< 0.0001*
Residual	0.0437	7	0.0062		
Lack of Fit	0.0156	3	0.0052	0.7378	0.5821 ^{ns}
Pure Error	0.0281	4	0.0070		
Cor Total	4.43	16			

A – fermentation time (days); B – initial media pH; C – initial moisture content (%)

*Significant (p-value <0.05); nsNot significant (p-value >0.05)

Moreover, the model F-values obtained were 68.17 for FPase activity and 78.16 for CMCase activity, indicating that the terms in the model have significant effects on cellulase activity (Peng et al. 2020). The probability of these F-values occurring due to noise is only 0.01%. Additionally, the Lack of Fit F-values were 2.39 and 3.07, respectively, which were not significant relative to the pure error. This result, with a 28.18% and 58.21% chance of occurring due to noise, respectively, suggests that the models fit the experimental data well.

The statistical evaluation of the model's goodness-of-fit was conducted, and the data are listed in Table 9 for the two models. The standard deviation for FPase activity was 0.0179 and 0.0790 for CMCase activity, indicating that the data points are closely clustered around their mean values. The coefficient of variations obtained (2.85% for FPase and 3.81% for CMCase) were within the acceptable limits of less than 5%, further indicating that the model has high precision and the variability in the data is minimal relative to the mean (Selvan et al. 2018).

Table 9: Regression analysis for the determination of the model's goodness-of-fit for predicting FPase and CMCase activity.

Source	Value	
	FPase activity	CMCase activity
Std. Dev.	0.0179	0.070
Mean	0.6295	2.08
C.V. %	2.85	3.81
R ²	0.9887	0.9901
Adjusted R ²	0.9742	0.9775
Predicted R ²	0.8881	0.9339
Adeq. Precision	23.0243	30.3275

The coefficient of determination (R²) was close to 1, demonstrating that 98.87% of the variability in cellulase production in terms of FPase activity can be explained by the model, while 99.01% of the variability in cellulase production in terms of CMCase activity can also be explained by the model. These high R² values signify an excellent fit between the model predictions and the actual experimental data. The difference between the Predicted R² and the Adjusted R² in each model is less than 0.2. This means that the former value is in reasonable agreement with the latter value due to their small difference (Sahoo 2011).

Although the predicted R², which assesses the model's predictive capability for new data, is slightly lower than the adjusted R², it still indicates that the model can reliably forecast cellulase production under different experimental conditions. Furthermore, the adequate precision values, representing the signal-to-noise ratio, were 23.0243 for FPase activity and 30.327 for CMCase activity. These values significantly exceed the recommended threshold of 4, demonstrating a strong signal and confirming the model's ability to efficiently explore the design space.

Considering the established relationship between the predicted and actual responses, the regression coefficients were fitted to a second-order polynomial equation to derive a coded equation that can be used to predict the response based on the levels of

$$\begin{aligned} \text{FPase activity } \left(\frac{U}{gds} \right) &= +0.7366 - 0.0225 (A) + 0.1028 (B) + 0.0483 (C) - 0.0150(AB) - 0.215 (AC) - 0.0080(BC) \\ &- 0.0820 (A^2) - 0.0460 (B^2) - 0.0995 (C^2) \end{aligned}$$

Equation 3

$$\begin{aligned} \text{CMCase activity } \left(\frac{U}{gds} \right) &= +2.50 - 0.2130 (A) + 0.4624 (B) + 0.3124 (C) - 0.2325(AB) - 0.0325 (AC) - 0.0138 (BC) \\ &- 0.2609 (A^2) - 0.2287 (B^2) - 0.4022 (C^2) \end{aligned}$$

Equation 4

where A is fermentation time (days); B is the initial media pH; and C is the initial moisture content.

Individual and interaction effects of independent factors on cellulase production

To study the individual effects of the independent factors on cellulase production, one-factor-at-a-time graphs were obtained from the Design-Expert® DX13 software. These results analyzed the effects of fermentation time, initial media pH, and initial moisture content on cellulase activity, measured in terms of filter paper (FPase) and carboxymethyl (CMCase) activity.

each factor. The coded mathematical equations in terms of experimental variables as determined by BBD are given in equations 3 and 4:

The effect of fermentation time on FPase activity and CMCase activity was depicted in a bell-shaped curve, as shown in Figures 2A and 3A, respectively, illustrating the relationship between fermentation time and cellulase activity. As the fermentation time progressed, the FPase and CMCase activities increased. The graph showed that the FPase activity reached its peak between day 5 and day 6, while the CMCase activity started to decline after day 4.

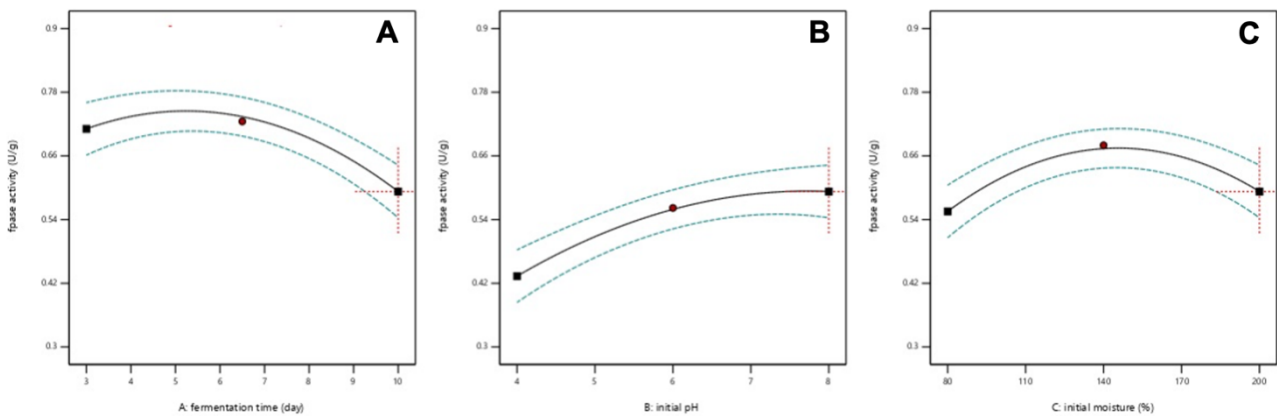


Figure 2: Effects of varying fermentation time (A), initial media pH (B), and initial moisture content (C) on the FPase activity.

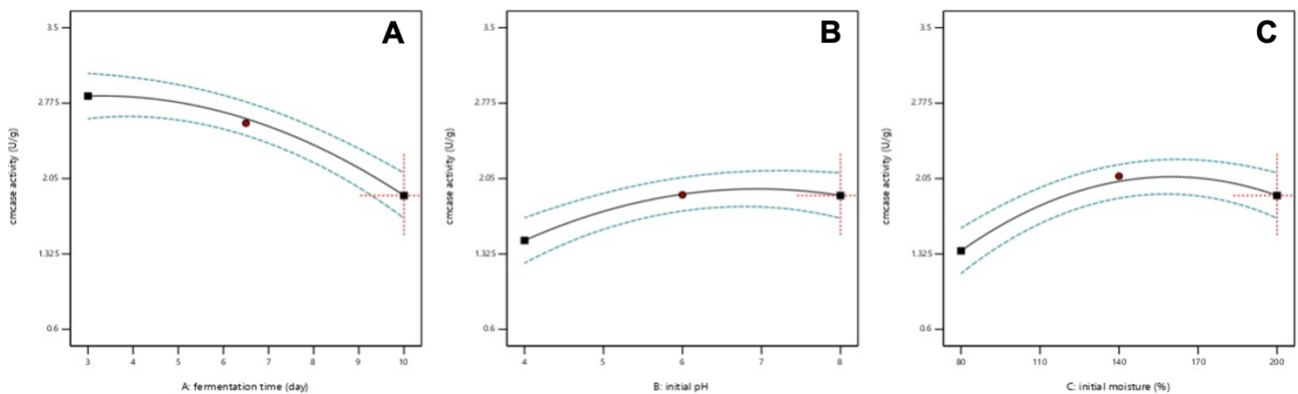


Figure 3: Effects of varying fermentation time (A), initial media pH (B), and initial moisture content (C) on the CMCase activity.

Figures 2B and 3B illustrate the influence of initial media pH on FPase and CMCase activities, demonstrating a positive correlation between these factors. This suggests that *T.*

asperelloides is capable of efficiently producing cellulase under higher or alkaline pH conditions. A similar pattern was observed with respect to initial moisture content, as shown in Figures 2C

and 3C, where the optimal moisture level for cellulase production was at the upper end of the tested range, highlighting the importance of adequate moisture for maximizing enzyme yield.

Additionally, the interactive effects of the independent variables on FPase and CMCase activities were examined through 3D surface plots, which were generated by varying two independent factors while keeping the third constant. The 3D surface curves and contour plots, depicting the interactions among the variables

for FPase and CMCase activities, are presented in Figures 4–9.

Figures 4–5 illustrate that the highest FPase and CMCase activities were achieved when the initial moisture content was at the central level (140%), whereas the lowest enzyme activity occurred at the lower moisture content (80%). This pattern underscores the role of increased moisture in improving nutrient transport and promoting fungal growth in solid-state fermentation, thereby enhancing enzyme production.

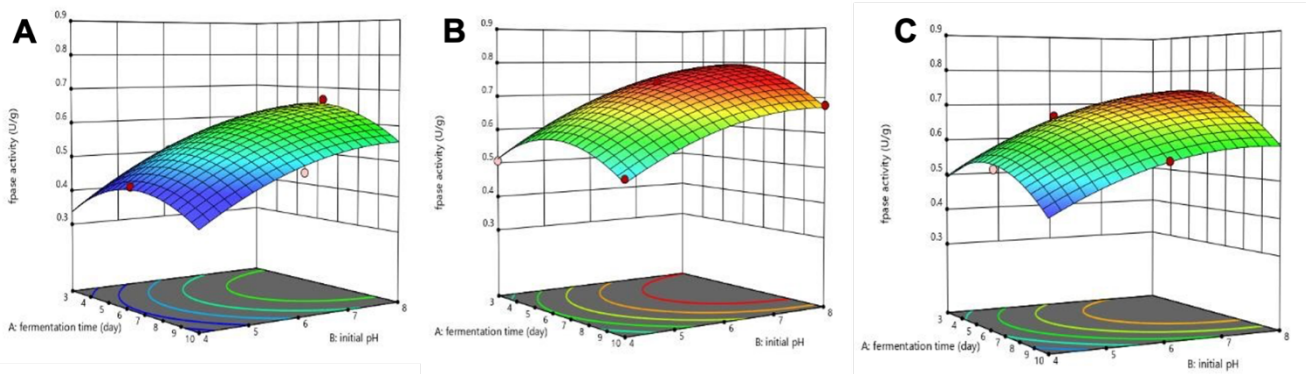


Figure 4: 3D surface graph for an interactive effect of fermentation time and initial media pH on FPase activity when initial moisture content is at (A) low, (B) central, and (C) high levels.

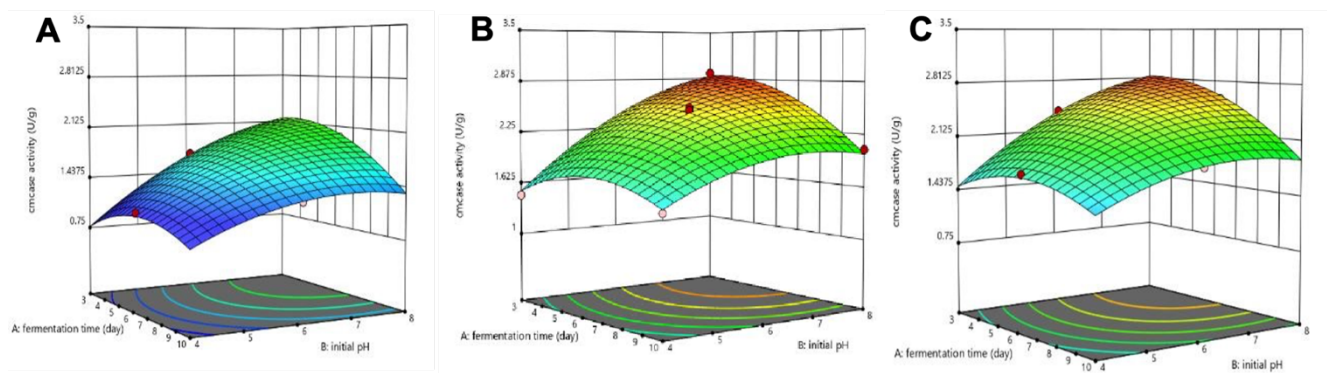


Figure 5: 3D surface graph for an interactive effect of fermentation time and initial media pH on CMCase activity when initial moisture content is at (A) low, (B) central, and (C) high levels.

Similar trends have been reported in other studies on SSF, where optimal moisture content is significant for maintaining the balance between substrate hydration and microbial activity (Kalsoom et al. 2019, Ortiz et al. 2015). However, in this study, the lowest initial moisture content set was 80% due to the high-water absorbing properties of the coconut coir. In addition, it was observed that substrate porosity and particle size may influence optimum moisture content.

Illustrated in Figures 6 and 7 are the interactive effects of fermentation time and initial moisture content when the initial media pH is at low, center, and high levels. The positive correlation between pH and enzyme activity suggests that *T.*

asperelloides RS1 prefers neutral to slightly alkaline conditions for optimal cellulase enzyme activity under SSF. This contrasts with several studies that reported the optimal pH for maximum cellulase activity by *Trichoderma* sp. is acidic, ranging from 3.0 to 6.0, when using pure cellulose as the carbon source (Juhasz et al. 2004, Ryu and Mandels 1980). Moreover, Delabona et al. (2012) showed that *T. harzianum* was also able to produce cellulase enzymes at pH 6.0 when using sugarcane bagasse as substrate. The observed difference in optimal pH can be attributed to the nature of the substrate and fermentation conditions.

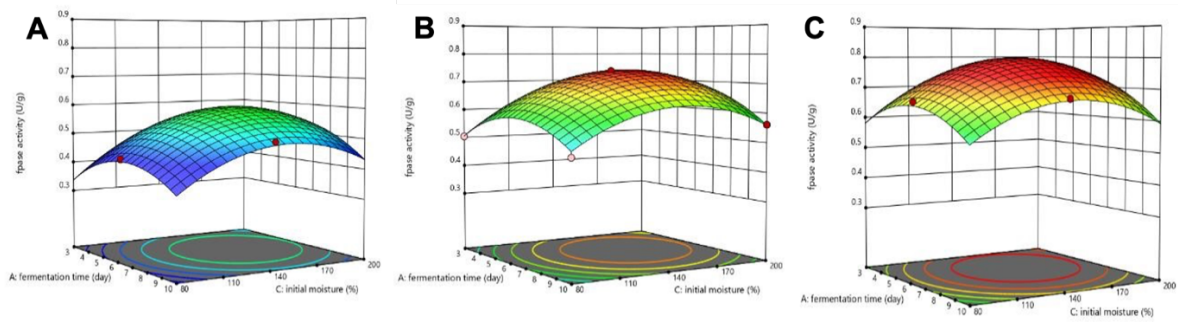


Figure 6: 3D surface graph for an interactive effect of fermentation time and initial moisture content on FPase activity when initial pH is at (A) low, (B) central, and (C) high levels.

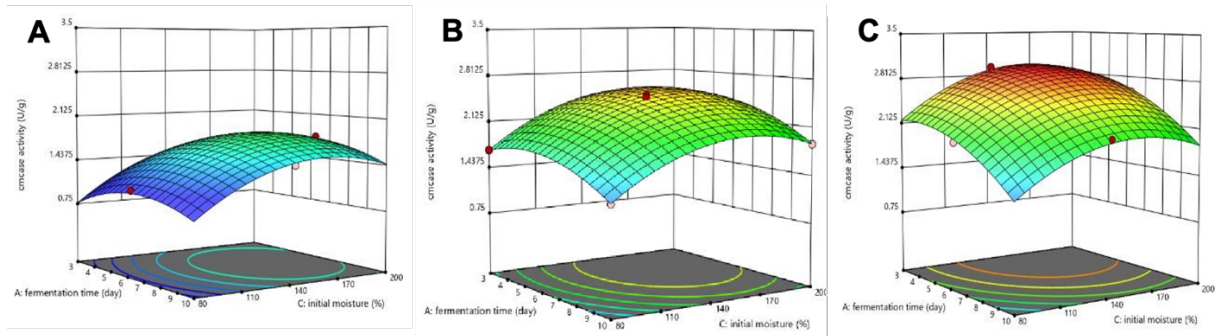


Figure 7: 3D surface graph for an interactive effect of fermentation time and initial moisture content on CMCase activity when B: initial pH is at (A) low, (B) central, and (C) high levels.

Figures 8 and 9 illustrate the effect of interactions between initial media pH and initial moisture content when fermentation time is at low, center, and high level on the FPase and CMCase activities. The enzyme activities showed a clear increasing trend as the fermentation time progressed, peaking between 5 and 6 days of fermentation. After reaching this peak, a noticeable decline in activity was observed. This suggests that the optimal fermentation period for maximum enzyme activity by *T. asperelloides* under the given conditions is around this period. This trend suggests that prolonged fermentation beyond this optimal point may lead to the depletion of nutrients or the accumulation of inhibitory by-products, which negatively affect the production of cellulase.

the enzyme activity of *Trichoderma* species generally increases with fermentation time, reaching an optimum before declining due to product inhibition (Thakur et al. 2023, Mrudula and Murugammal 2011). This decrease in activity is likely caused by the accumulation of cellobiose, a byproduct of cellulose hydrolysis, which inhibits the activities of CMCase and FPase by competing with cellulose for the enzyme's active site (Ojumu and Betiku 2003). In addition, phenolic compounds released from residual lignin during hydrolysis may further suppress cellulase activity (Qin et al. 2016). Enzyme denaturation, potentially due to interactions with other substances present in or released from the substrate, could also contribute to the observed reduction in enzyme efficiency (Ramesh and Lonsane 1987).

This trend is consistent with findings from other studies, where

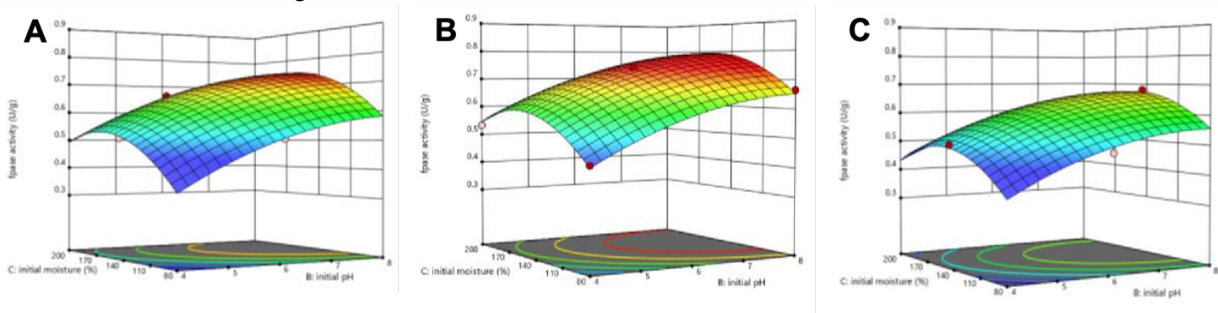


Figure 8: 3D surface graph for an interactive effect of initial media pH and initial moisture content on FPase activity when fermentation time is at (A) low, (B) central, and (C) high levels.

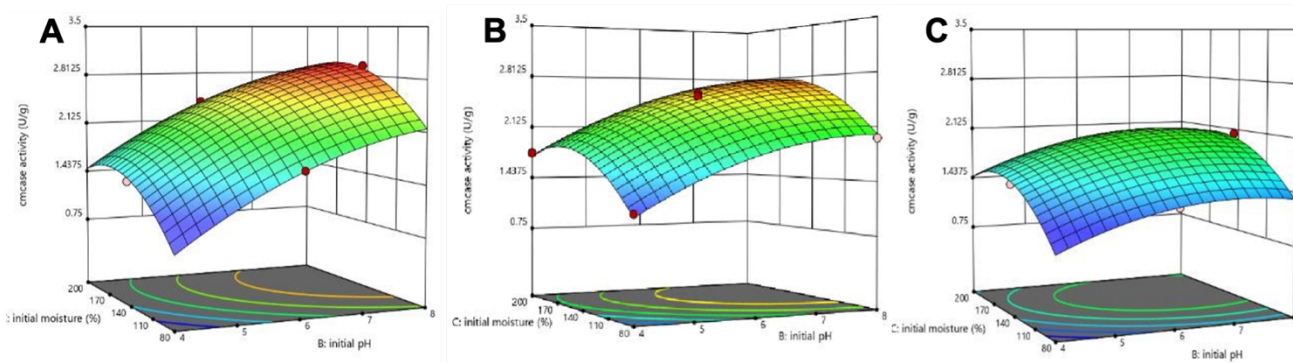


Figure 9: 3D surface graph for an interactive effect of initial media pH and initial moisture content on CMCase activity when fermentation time is at (A) low, (B) central, and (C) high levels.

Confirmation of the generated model for the optimization of cellulase activity

For optimum CMCase and FPase activities, various combinations of experimental factors were generated through numerical optimization following the analysis of responses. The software provided 100 solutions, all with 1.000 desirability, and a random solution was chosen for verification having the following fermentation conditions: 3.6 fermentation days, an initial media pH of 7.88, and 163.71% moisture content.

Upon experimental validation of the optimum generated model, the average FPase and CMCase activities were found to be 0.770 U/gds and 2.919 U/gds, respectively, which corresponds to a percent error of 0.74% and 2.9%. Both have a low standard deviation implying that the experimental values are clustered tightly around their mean value.

Table 10: Percent error of FPase activity (U/gds) from the selected optimized fermentation conditions.

Trial	Predicted FPase Activity, U/gds	Experimental FPase Activity, U/gds	Percent Error
1		0.7686	0.73
2	0.7742	0.7648	1.23
3		0.7686	0.24
Mean		0.7698 ± 0.0057	0.74 ± 0.0049

Table 11: Percent error of CMCase activity (U/gds) from the selected optimized fermentation conditions.

Trial	Predicted CMCase Activity, U/gds	Experimental CMCase Activity, U/gds	Percent Error
1		2.9033	2.38
2	2.9724	2.8958	2.65
3		2.9585	0.47
Mean		2.9192 ± 0.0342	1.83 ± 0.0119

Potential sources of error include fluctuations in environmental conditions, such as temperature and humidity, as the setup was not conducted in an incubator to precisely control incubation temperature. Additionally, minor inaccuracies in measuring the initial moisture content and pH, along with biological variability in fungal growth and enzyme production, may have contributed to discrepancies between the predicted and actual values. The physical properties of the coconut coir fibers, such as the particle size, could also contribute to the observed deviation between predicted and experimental cellulase activity. Differences in fiber size may influence the surface area available for microbial colonization, affecting fermentation efficiency and enzyme production. Despite these deviations, the overall mean percent error remains low, indicating that the optimized conditions provide reproducible cellulase activities within acceptable limits under the experimental conditions tested.

CONCLUSION

This study highlights the first report of *Trichoderma asperelloides* RS1 isolated from rice straw to produce cellulase via SSF using coconut coir as substrate. RSM optimization was done to investigate three independent factors, namely initial media pH, initial moisture content, and fermentation time, that could affect enzyme production under SSF. By analyzing the response surfaces and contour plots, this study generated a quadratic model to predict the most favorable combination of initial media pH, initial moisture content, and fermentation period for maximizing cellulase yield. The FPase activity was

found to be optimal when the initial media pH, initial moisture content, and fermentation time were pH 6.0, 140%, and 6.5 days, respectively, yielding 0.762 U_{glc}/gds. On the other hand, the fermentation conditions for maximum CMCase activity are at day 3 of fermentation with an initial media pH of 8.0 and a moisture content of 140%, which yielded 2.951 U_{glc}/gds. Validation of the predicted optimum models yielded 0.74% and 2.9% errors for FPase and CMCase activities, respectively. The results presented in this study showed the potential of *T. asperelloides* RS1 to produce cellulase from coconut coir under optimized solid-state fermentation. It is recommended for future studies to investigate pretreatment methods for coconut coir in order to reduce lignin content, which could possibly enhance cellulose accessibility, thereby increasing enzyme yield. Additionally, expanding the optimization parameters to include other factors as well as scale-up studies that yield cellulase in larger quantities suitable for industrial applications.

ACKNOWLEDGMENT

The authors would like to acknowledge the Feeds and Specialty Products Laboratory, National Institute of Molecular Biology and Biotechnology (BIOTECH), and the Institute of Chemistry, University of the Philippines Los Baños, for the use of facilities and equipment in the conduct of this research.

CONFLICT OF INTEREST

All the authors have no conflict of interest to declare.

CONTRIBUTIONS OF INDIVIDUAL AUTHORS

NGDumandan, SLBArreola, and AAYanos conceptualized and supervised the study. JMAMinion, LJFLabitag, and ACTKagaoan conducted laboratory experiments. All authors analyzed the data, wrote the initial draft, and approved the final version of the manuscript.

DATA AVAILABILITY

Datasets related to this article will be made available upon request.

FUNDING SUPPORT

This research did not receive any specific grant from funding agencies in the public, commercial, or not-for-profit sectors.

REFERENCES

- Abu YN, Barrena R, Komilis D, Sánchez A. Solid-state fermentation as a novel paradigm for organic waste valorization: A review. *Sustainability* 2017; 9(2):224. <https://doi.org/10.3390/su9020224>
- Ahmad T, Sharma A, Gupta G, Mansoor S, Jan S, Kaur B, Paray BA, Ahmad A. Response surface optimization of cellulase production from *Aneurinibacillus aneurinilyticus* BKT-9: An isolate of urban Himalayan freshwater. *Saudi Journal of Biological Sciences* 2020; 27(9):2333–2343. <https://doi.org/10.1016/j.sjbs.2020.04.036>
- Ahmed A, Bibi A. Fungal cellulase; production and applications: Mini-review. *Life International Journal of Health Life Sciences* 2018; 4(1):19–36. <https://doi.org/10.20319/ijhls.2018.41.1936>
- Ali B, Hawreen A, Kahla NB, Amir MT, Azab M, Raza A. A critical review on the utilization of coir (coconut fiber) in cementitious materials. *Construction and Building Materials* 2022; 351:128957. <https://doi.org/10.1016/j.conbuildmat.2022.128957>
- Arja MO. Cellulases in the textile industry. In: Polaina J, MacCabe AP, editors. *Industrial Enzymes*. Springer; 2007. p. 51–63. https://doi.org/10.1007/1-4020-5377-0_4
- Awotwe-Otoo D, Agarabi C, Faustino PJ, Habib MJ, Lee S, Khan MA, Shah RB. Application of quality by design elements for the development and optimization of an analytical method for protamine sulfate. *Journal of Pharmaceutical and Biomedical Analysis* 2012; 62:61–67. <https://doi.org/10.1016/j.jpba.2012.01.002>
- Béguin P, Aubert J. The biological degradation of cellulose. *FEMS Microbiology Reviews* 1994; 13(1):25–58. <https://doi.org/10.1111/j.1574-6976.1994.tb00033.x>
- Bulgari D, Alias C, Peron G, Ribaudo G, Gianoncelli A, Savino S, Bouregghda H, Bouznad Z, Monti E, Gobbi E. Solid-state fermentation of *Trichoderma* spp.: A new way to valorize agricultural digestate and produce value-added bioproducts. *Journal of Agricultural and Food Chemistry* 2023; 71(9):3994–4004. <https://doi.org/10.1021/acs.jafc.2c07388>
- Campos AO, Asevedo EA, Souza Filho PF, Santos ES dos. Extraction of cellulases produced through solid-state fermentation by *Trichoderma reesei* CCT-2768 using green coconut fibers pretreated by steam explosion combined with alkali. *Biomass* 2024; 4(1):92–106. <https://doi.org/10.3390/biomass4010005>
- Chen L. *Trichoderma* cf. *asperelloides* strain z4-1 small subunit ribosomal RNA gene, partial sequence; internal transcribed spacer 1, 5.8S ribosomal RNA gene, and internal transcribed spacer 2, complete sequence; and large subunit ribosomal RNA gene, partial sequence [Accession No. OP821901.1]. GenBank. <https://www.ncbi.nlm.nih.gov/nucleotide/OP821901.1>
- Delabona PS, Farinas CS, da Silva MR, Azzoni SF, Pradella JG. Use of a new *Trichoderma harzianum* strain isolated from the Amazon rainforest with pretreated sugar cane bagasse for on-site cellulase production. *Bioresour Technol* 2012; 107:517–521. <https://doi.org/10.1016/j.biortech.2011.12.048>
- Druzhinina IS, Chenthamara K, Zhang J, Atanasoa L, Yang D, et al. Massive lateral transfer of genes encoding plant cell wall-degrading enzymes to the mycoparasitic fungus *Trichoderma* from its plant-associated hosts. *PLoS Genet* 2018; 14(4). <https://doi.org/10.1371/journal.pgen.1007322>
- Ejaz U, Sohail M, Ghanemi A. Cellulases: From Bioactivity to a Variety of Industrial Applications. *Biomimetics* 2021; 6(3):44. <https://doi.org/10.3390/biomimetics6030044>
- El Baz AF, Shetaia YMH, Shams Eldin HA, ElMekawy A. Optimization of Cellulase Production by *Trichoderma viride* Using Response Surface Methodology. *Curr Biotechnol* 2018; 7(1):19–25. <https://doi.org/10.2174/2211550105666160115213402>
- Gashe BA. Cellulase production and activity by *Trichoderma* sp. A-001. *J Appl Bacteriol* 1992; 73(1):79–82. <https://doi.org/10.1111/j.1365-2672.1992.tb04973.x>
- Ghose TK. Cellulase biosynthesis and hydrolysis of cellulosic substances. In: Ghose TK, Fiechter A, Blakebrough N, editors. *Advances in Biochemical Engineering, Volume 6*. Springer Berlin Heidelberg; 1977. p. 39–76. https://doi.org/10.1007/3-540-08363-4_2
- Guruk M, Karaaslan M. Production and Biochemical Characterization of Cellulase Enzyme by *Trichoderma* Strains from Harran Plain. *Int J Life Sci Biotechnol* 2020; 3(3):258–274. <https://doi.org/10.38001/ijlsb.756818>
- Hind L, Zahia M, Hayet BL, Estelle C, Francis D. Production and characterization of cellulolytic activities produced by *Trichoderma longibrachiatum* (GHL). *Afr J Biotechnol* 2013; 12(5):465–475. <https://doi.org/10.5897/AJB12.917>
- Hölker U, Höfer M, Lenz J. Biotechnological advantages of laboratory-scale solid-state fermentation with fungi. *Appl Microbiol Biotechnol* 2004; 64(2):175–186. <https://doi.org/10.1007/s00253-003-1504-3>
- Jayasekara S, Ratnayake R. Microbial Cellulases: An Overview and Applications. In: Rodríguez Pascual A, Eugenio Martín

- ME, editors. Cellulose. IntechOpen; 2019. <https://doi.org/10.5772/intechopen.84531>.
- Juhász T, Szengyel Z, Szijártó N, Réczey K. Effect of pH on Cellulase Production of *Trichoderma reesei* RUT C30. In: Finkelstein M, McMillan JD, Davison BH, Evans BH, editors. Proceedings of the Twenty-Fifth Symposium on Biotechnology for Fuels and Chemicals Held May 4–7, 2003, in Breckenridge, CO. Biotechnology for Fuels and Chemicals. Humana Press, Totowa, NJ; 2004. https://doi.org/10.1007/978-1-59259-837-3_18.
- Kaloom R, Ahmed S, Nadeem M, Chohan S, Abid M. Biosynthesis and extraction of cellulase produced by *Trichoderma* on agro-wastes. Int J Environ Sci Technol 2019; 16(2):921–928. <https://doi.org/10.1007/s13762-018-1717-8>.
- Keshavarz B, Khalesi M. *Trichoderma reesei*, a superior cellulase source for industrial applications. Biofuels 2016; 7(6):713–721. <https://doi.org/10.1080/17597269.2016.1192444>.
- Khalil HPSA, Alwani MS, Omar AKM. Chemical composition, anatomy, lignin distribution, and cell wall structure of Malaysian plant waste fibers. BioResources 2006; 1(2):220–232. <https://doi.org/10.15376/biores.1.2.220-232>.
- Krishna C. Production of bacterial cellulases by solid-state bioprocessing of banana wastes. Bioresour Technol 1999; 69(3):231–239. [https://doi.org/10.1016/S0960-8524\(98\)00193-X](https://doi.org/10.1016/S0960-8524(98)00193-X).
- Kuhad RC, Gupta R, Singh A. Microbial cellulases and their industrial applications. Enzyme Res 2011; 2011:1–10. <https://doi.org/10.4061/2011/280696>.
- Kumar M, Tiwari S, Manohar S, Singh RK, Kumar R, Srivastava S. Solid-state fermentation of agricultural wastes for cellulase production by *Trichoderma viride*. Environ Technol Innov 2021; 21:101248. <https://doi.org/10.1016/j.eti.2020.101248>.
- Lama-Muñoz A, Martín-Martínez H, Vergara-Barberán M, Garrido-Fernández A, Fernández-Bolaños J, Rodríguez-Gutiérrez G. Production, characterization, and antioxidant activity of bioactive extracts rich in fiber and phenolics obtained from winery and olive oil wastes by efficient enzyme-assisted extraction. Foods 2019; 8(7):246. <https://doi.org/10.3390/foods8070246>.
- Li Y-H, Ding M, Wang J-H, Xu G-R, Zhao F, Chi Z-M. Efficient production of raw-starch-digesting enzyme, acidic amylase, and cellulase by the marine yeast *Aureobasidium pullulans* N13d in sea water-based medium. Appl Biochem Biotechnol 2015; 175(6):2720–2736. <https://doi.org/10.1007/s12010-014-1426-0>.
- Lynd LR, Weimer PJ, van Zyl WH, Pretorius IS. Microbial cellulose utilization: Fundamentals and biotechnology. Microbiol Mol Biol Rev 2002; 66(3):506–577. <https://doi.org/10.1128/MMBR.66.3.506-577.2002>.
- Ma Y, Liu Y, Burns CM, Sun L. Development of novel microbial platforms for the bioconversion of renewable resources into desired products. Renew Sustain Energy Rev 2020; 115:109393. <https://doi.org/10.1016/j.rser.2019.109393>.
- Mamma D, Kourtoglou E, Christakopoulos P. Fungal multienzyme production on industrial by-products of the citrus-processing industry. Bioresour Technol 2008; 99(7):2373–2383. <https://doi.org/10.1016/j.biortech.2007.05.008>.
- Mawadza C, Hatti-Kaul R, Zvauya R, Mattiasson B. Purification and characterization of cellulases produced by two *Bacillus* strains. J Biotechnol 2000; 83(3):177–187. [https://doi.org/10.1016/S0168-1656\(00\)00301-9](https://doi.org/10.1016/S0168-1656(00)00301-9).
- Mohana S, Shah A, Divecha J, Madamwar D. Xylanase production by *Burkholderia* sp. DMAX strain under solid state fermentation using distillery spent wash. Bioresour Technol 2008; 99(16):7553–7564. <https://doi.org/10.1016/j.biortech.2008.02.009>.
- Ouedraogo J-P, Tsang A. Production of Native and Recombinant Enzymes by Fungi for Industrial Applications. In: Zaragoza Ó, Casadevall A, editors. Encyclopedia of Mycology. Elsevier; 2021. p. 222–32. <https://doi.org/10.1016/B978-0-12-819990-9.00046-9>.
- Peij NNME van, Gielkens MMC, Vries RP de, Visser J, Graaff LH de. The Transcriptional Activator XlnR Regulates Both Xylanolytic and Endoglucanase Gene Expression in *Aspergillus niger*. Appl Environ Microbiol 1998; 64(10):3615–9. <https://doi.org/10.1128/AEM.64.10.3615-3619.1998>.
- Pérez-Guerra N, Torrado-Agrasar A, López-Macias C, Pastrana L. Main characteristics and applications of solid substrate fermentation. Electron J Environ Agric Food Chem 2003; 2(3):343–50. <https://doi.org/10.5618/ejeafche.2003.v2i3.98>.
- Qin M, Xia H, Zou G, Li X, Zeng B, et al. Integrated transcriptomics and proteomics analyses of *Trichoderma reesei* under light-dark cyclic conditions and implications for cellulase production. Sci Rep 2018; 8(1):10690. <https://doi.org/10.1038/s41598-018-29094-0>.
- Raghuwanshi S, Deswal D. Cellulase enzyme: structure and applications. Int J Curr Microbiol Appl Sci 2014; 3(5):573–9.
- Rajyalakshmi I, Veerabhadra Rao A, Babu Potti R. *Trichoderma asperelloides* isolate STAL small subunit ribosomal RNA gene, partial sequence; internal transcribed spacer 1, 5.8S ribosomal RNA gene, and internal transcribed spacer 2, complete sequence; and large subunit ribosomal RNA gene, partial sequence [Accession No. MH371292.1]. GenBank. <https://www.ncbi.nlm.nih.gov/nuccore/MH371292.1>.
- Ravindran R, Jaiswal S, Abu-Ghannam N, Jaiswal AK. A comparative analysis of pretreatment strategies on the properties and hydrolysis of brewers' spent grain. Bioresour Technol 2018; 248:272–9. <https://doi.org/10.1016/j.biortech.2017.06.009>.
- Rekadwad BN, Pathak SP. Fungal cellulases: Sources and Applications. In: Ramos HL, Ribeiro PA, editors. Fungal Biotechnology and Bioengineering. Springer International Publishing; 2017. p. 185–202. https://doi.org/10.1007/978-3-319-48432-1_11.
- Robbertse B, Strope PK, Chaverri P, Gazis R, Ciufu S, Domrachev M, Schoch CL. *Trichoderma reesei* ITS region; from TYPE material [Accession No. NR_120297.1]. GenBank. https://www.ncbi.nlm.nih.gov/nuccore/NR_120297.1.
- Robbertse B, Strope PK, Chaverri P, Gazis R, Ciufu S, Domrachev M, Schoch CL. *Trichoderma compactum* YMF 1.01693 ITS region; from TYPE material [Accession No.

- NR_138435.1]. GenBank.
https://www.ncbi.nlm.nih.gov/nuccore/NR_138435.1.
- Robbertse B, Strope PK, Chaverri P, Gazis R, Ciuffo S, Domrachev M, Schoch CL. *Trichoderma pseudolacteum* TMI 8484 ITS region; from TYPE material [Accession No. NR_134436.1]. GenBank.
https://www.ncbi.nlm.nih.gov/nuccore/NR_134436.1.
- Sahin HT, Arslan MB. A study on physical and chemical properties of cellulose paper immersed in various solvent mixtures. *Int J Mol Sci* 2008; 9(1):78–88.
<https://doi.org/10.3390/ijms9010078>.
- Sánchez A, Demain AL. Metabolic regulation of cellulase and xylanase formation by *T. reesei*. In: Du TT, editor. *Biotechnology for Biofuels Production and Optimization*. Springer; 2008. p. 139–52. https://doi.org/10.1007/978-1-4020-8243-6_10.
- Schoch CL, Robbertse B, Robert V, Vu D, Cardinali G, et al. *Aspergillus niger* ATCC 16888 ITS region; from TYPE material [Accession No. NR_111348.1]. GenBank.
https://www.ncbi.nlm.nih.gov/nuccore/NR_111348.1.
- Shelke DB, Holkar SK, Ghotgalkar PS, Bhanbhane VC, Shewale SA, Saha S. *Trichoderma asperellum* isolate Manik Chaman (TMCR1) small subunit ribosomal RNA gene, partial sequence; internal transcribed spacer 1, 5.8S ribosomal RNA gene, and internal transcribed spacer 2, complete sequence; and large subunit ribosomal RNA gene, partial sequence [Accession No. OM280457.1]. GenBank.
<https://www.ncbi.nlm.nih.gov/nuccore/OM280457.1>.
- Srivastava N, Srivastava M, Mishra PK, Gupta VK, Molina G, Rodriguez-Couto S, Manikanta A, Ramteke PW. Applications of fungal cellulases in biofuel production: Advances and limitations. *Renew Sustain Energy Rev* 2018; 82:2379–86.
<https://doi.org/10.1016/j.rser.2017.08.074>.
- Sukumaran RK, Singhania RR, Mathew GM, Pandey A. Cellulase production using biomass feedstock and its application in lignocellulose saccharification for bio-ethanol production. *Renew Energy* 2009; 34(2):421–4.
<https://doi.org/10.1016/j.renene.2008.05.008>.
- Tomás-Pejó E, García-Aparicio M, Negro MJ, Oliva JM, Ballesteros M. Effect of different cellulase dosages on cell viability and ethanol production by *Kluyveromyces marxianus* in SSF processes. *Bioresour Technol* 2009; 100(2):890–5.
<https://doi.org/10.1016/j.biortech.2008.07.012>.
- Várnai A, Siika-aho M, Viikari L. Restriction of the enzymatic hydrolysis of steam-pretreated spruce by lignin and hemicellulose. *Enzyme Microb Technol* 2010; 46(3–4):185–93. <https://doi.org/10.1016/j.enzmictec.2009.12.013>.
- Zhang Y-H P, Lynd L R. Toward an aggregated understanding of enzymatic hydrolysis of cellulose: Noncomplexed cellulase systems. *Biotechnol Bioeng* 2004; 88(7):797–824.
<https://doi.org/10.1002/bit.20282>.
- Zhou J, Wang J, Bai X, Fang W. Study of cellulase production and enzymatic properties of *Penicillium oxalicum* GZ-2. *Biotechnol Bioequip* 2017; 31(1):152–8.
<https://doi.org/10.1080/13102818.2016.1269313>.